



Geophysical Research Letters

RESEARCH LETTER

10.1029/2018GL079223

Special Section:

The Arctic: An AGU Joint Special Collection

Key Points:

- Winter Arctic sea ice thickness and growth variability is explored using data from climate models and satellite observations
- We project an increase in winter Arctic sea ice growth over the coming decades, due in-part to the presence of a negative conductive feedback associated with thinner ice
- The importance of the negative feedback reduces through the end of the 21st century, as the Arctic warms significantly and promotes delays and overall declines in Arctic sea ice growth

Supporting Information:

- Supporting Information S1

Correspondence to:

A. A. Petty,
alek.a.petty@nasa.gov

Citation:

Petty, A. A., Holland, M. M., Bailey, D. A., & Kurtz, N. T. (2018). Warm Arctic, increased winter sea ice growth? *Geophysical Research Letters*, *45*, 12,922–12,930. <https://doi.org/10.1029/2018GL079223>

Received 14 JUN 2018

Accepted 29 SEP 2018

Accepted article online 4 OCT 2018

Published online 6 DEC 2018

Warm Arctic, Increased Winter Sea Ice Growth?

Alek A. Petty^{1,2} , Marika M. Holland³ , David A. Bailey³ , and Nathan T. Kurtz

¹Cryospheric Sciences Laboratory, NASA Goddard Space Flight Center, Greenbelt, MD, USA, ²Earth System Science Interdisciplinary Center, University of Maryland, College Park, MD, USA, ³National Center for Atmospheric Research, Boulder, CO, USA

Abstract We explore current variability and future projections of winter Arctic sea ice thickness and growth using data from climate models and satellite observations. Winter ice thickness in the Community Earth System Model's Large Ensemble compares well against thickness estimates from the Pan-Arctic Ice Ocean Modeling and Assimilation System and CryoSat-2, despite some significant regional differences—for example, a high thickness bias in Community Earth System Model's Large Ensemble in the western Arctic. Differences across the available CryoSat-2 thickness products hinder more robust validation efforts. We assess the importance of the negative conductive feedback of sea ice growth (thinner ice grows faster) by regressing October atmosphere/ice/ocean conditions against winter ice growth. Our regressions demonstrate the importance of a strong negative conductive feedback process in our current climate, which increases winter growth for thinner initial ice, but indicate that later in the 21st century this negative feedback is overwhelmed by variations in the fall atmosphere/ocean state.

Plain language summary In this study we explore the thickness and growth of Arctic sea ice through winter using data from climate models and satellite observations. Winter Arctic sea ice thickness in a widely used set of climate model simulations compares well against thickness estimates produced from a climate model constrained by observations and sea ice thickness estimates derived from satellite observations, although important regional differences are found. Our analysis suggests an increase in the amount of Arctic sea ice grown in winter through the coming decades, partly due to the fact thinner ice grows faster than thicker, more insulated, ice. As the Arctic warms rapidly, the strong atmosphere and ocean forcing dominates over this feedback and is projected to promote declines in sea ice growth.

1. Introduction

Arctic sea ice grows in extent and thickness during fall and winter, while the return of solar radiation and increases in air temperature promote sea ice melt through spring and summer. Rapid changes in the Arctic climate system over the last several decades have pushed this seasonal cycle out of balance—sea ice is melting more than it is growing—causing a well reported decline in total Arctic sea ice volume (Kwok & Rothrock, 2009; Lindsay & Schweiger, 2015). Myriad processes contribute to sea ice growth and melt, with arguably more attention given to sea ice melt processes given the more rapid declines observed in summer, and ongoing debates around the timing of an ice-free Arctic (e.g., Notz & Marotzke, 2012; Notz & Stroeve, 2016; Perovich et al., 2007; Stroeve et al., 2011; Tsamados et al., 2015). However, recent winters in the Arctic have featured record high air temperatures and record low sea ice conditions (e.g., Boisvert et al., 2016; Cullather et al., 2016; Graham et al., 2017; Petty et al., 2018), motivating increased discussion of winter Arctic sea ice thickness and growth variability (e.g., Ricker, Hendricks, Girard-Ardhuin, et al., 2017; Stroeve et al., 2018). Reductions in end of winter ice volume can also precondition the ice pack for enhanced summer ice loss, increasing the potential for new record low summer minima and a possible ice-free Arctic.

Improved assessments of winter Arctic sea ice thickness and growth are also needed due to their importance to the global climate system. For example, brine rejection during sea ice formation modulates the upper ocean/mixed layer properties of the Arctic Ocean (AO) and can promote dense water formation, especially in the more weakly stratified North Atlantic sector of the Arctic (e.g., Polyakov et al., 2017). The state of the upper ocean is a critical factor determining the biogeochemical balance of the Arctic and sub-Arctic system (e.g., Carmack et al., 2016).

The recent study of Stroeve et al. (2018) explored winter Arctic ice thickness variability and highlighted the importance of the negative feedback of sea ice growth—thinner ice grows faster than thicker ice due to

its decreased insulation. This study also alluded to a possible decline in the strength of this negative feedback process over recent years. While the physical mechanism underlying this negative thickness feedback is relatively well understood (e.g., Bitz & Roe, 2004), its significance to the overall Arctic sea ice mass balance is still relatively uncertain. The significance of this feedback process has also likely changed considering the rapid declines in Arctic sea ice thickness over recent decades, and while future projections in the overall sea ice mass budgets from climate models have been considered (Holland et al., 2010), the controls on projected sea ice growth rates have not explicitly been addressed.

In this study we seek to better assess the relative importance of the negative feedback between start of winter Arctic sea ice thickness and total winter ice growth for recent decades and through the 21st century.

2. Data and Methods

We primarily make use of data from the Community Earth System Model (CESM) Large Ensemble (LE; Kay et al., 2015). The CESM-LE is based on the fully coupled CESM1.1 (Hurrell et al., 2013), which includes the Los Alamos sea ice model component CICE v4 (Hunke & Lipscomb, 2010) with some additions: more sophisticated melt pond physics, a new multiple scattering radiation transfer scheme, and aerosol deposition and cycling in the sea ice (Holland et al., 2012). CESM-LE was established to provide a consistent and accessible ensemble of model simulations to assess internal climate variability (Kay et al., 2015). The CESM-LE consists of 40 ensemble members and is forced with historical data from 1920 to 2005 and projected forcings from 2005 onward using the RCP8.5 climate forcing scenario. Here we use monthly data from the 40 ensemble members from 1980 to 2080. This 100-year period enables us to assess decadal-scale variability in ice growth and includes temporal overlap with our thickness validation data sets. Arctic sea ice in CESM-LE is broadly consistent with the mean Arctic sea ice thickness state as inferred from observational estimates from satellite altimetry (Jahn et al., 2016; Labe et al., 2018). We provide further comparisons between CESM-LE and satellite altimetry-derived thickness/growth estimates in this study using multiple satellite-derived thickness products (described later in this section).

We use the monthly CESM-LE output of ice thickness from the start and end of winter (October and April respectively), the thermodynamic ice growth from October to April (the mean dynamic ice growth is also shown later), and snow thickness and ice concentration in October and April to characterize the winter sea ice state. To assess the strength of the winter atmospheric forcing we use monthly output of air temperature and specific humidity (both at 2-m reference height) and downwelling longwave radiation. To briefly assess the role of the ocean, we also use the monthly output of sea surface temperature. While Stroeve et al. (2018) chose November–April as the nominal growth season, we extend this back to October, as significant parts of the Arctic are expected to be undergoing freezeup during this month (Markus et al., 2009).

To explore the relationship between the start of winter ice thickness and winter ice growth we correlate the October to April thermodynamic ice growth (excluding the dynamical ice growth) with the October ice state (ice thickness, ice concentration, and snow thickness), and atmospheric forcing (air temperature, humidity, and downwelling longwave radiation). The correlations are calculated using a sliding 10-year window from all 40 individual ensemble members from 2011 to 2075 to assess current and future projections in these correlations in the CESM-LE. We also correlate the October ice/atmosphere state with the April ice thickness, to highlight the differences between ice growth and end of winter thickness variability.

We compare the CESM-LE results with thickness estimates obtained from the Pan-Arctic Ice-Ocean Modeling and Assimilation System (PIOMAS, v2.1; Zhang & Rothrock, 2003). PIOMAS is an ice-ocean model, producing ice thickness estimates constrained predominantly by the assimilation of sea ice concentration and sea surface temperature. PIOMAS ice thickness estimates show differences on the order of tens of centimeters compared to satellite-derived estimates, although this depends strongly on the time period and region analyzed (Schweiger et al., 2011; Zygmuntowska et al., 2014). We use the monthly October and April thickness data from 1980 to 2015.

We also compare the CESM-LE and PIOMAS thickness estimates with thickness data obtained from the European Space Agency's CryoSat-2 (CS-2) radar altimeter, which was launched in April 2010 (Wingham et al., 2006). CS-2 provides estimates of freeboard, the extension of sea ice above sea level, which can be

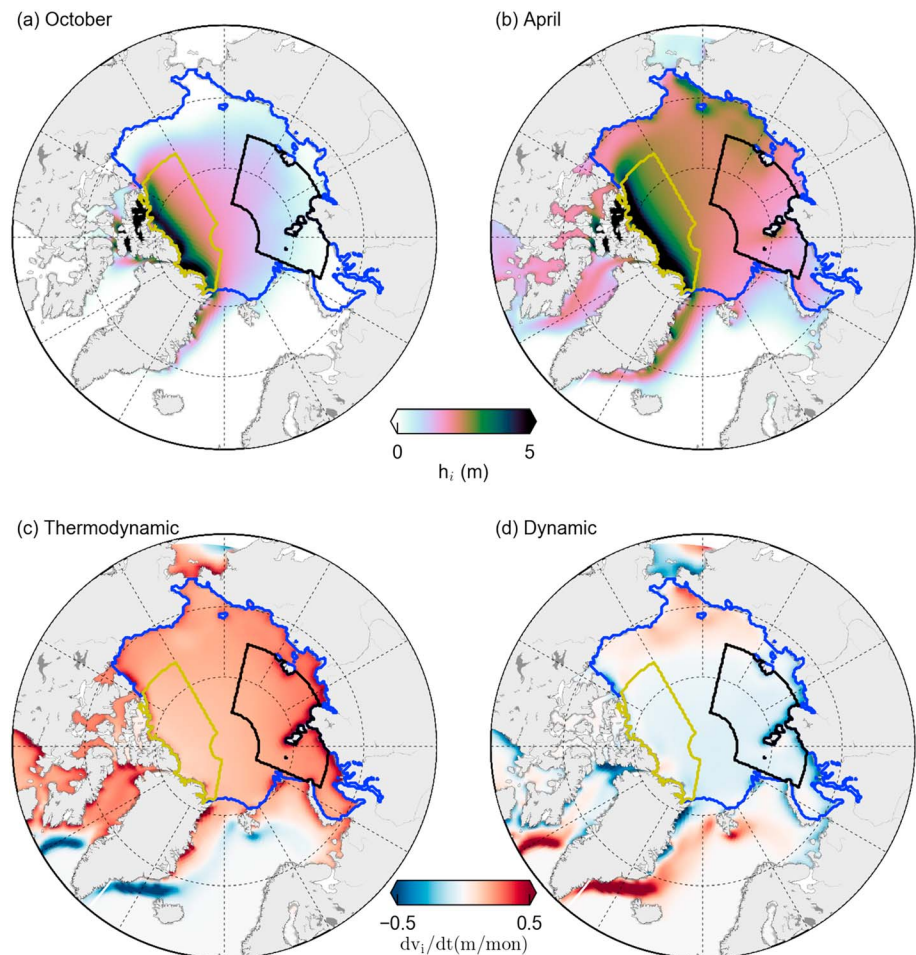


Figure 1. Mean (2006–2020) Arctic Sea ice thickness in (top left) October and (top right) April and (bottom left) October–April sea ice growth from thermodynamics and (bottom right) dynamics in the Community Earth System Model Large Ensemble simulations. The yellow, black, and blue boxes show the Western Arctic, Eastern Arctic, and Arctic Ocean domains, respectively.

converted to ice thickness using assumptions regarding snow depth, the snow and ice density, and hydrostatic equilibrium. Several international groups currently generate CS-2 thickness estimates, so we use data from National Aeronautics and Space Administration's (NASA) Goddard Space Flight Center (GSFC; Kurtz & Harbeck, 2017), the Center for Polar Observation and Modeling (CPOM; Tilling et al., 2017), and the Alfred Wegener Institute (AWI; Ricker, Hendricks, Kaleschke, et al., 2017). Differences in the CS-2 thickness data sets are largely driven by differences in the retracking of the radar returns, meaning the spread between the products represent to some degree the present uncertainty in the observational record. Note that the AWI thickness product also incorporates thin ice estimates from ESA's Soil Moisture and Ocean Salinity mission. To be consistent in our comparisons with CESM-LE, we set all open water or masked values to zero ice thickness. This was seen to be more consistent for our purposes than the alternative approach of using an ice thickness threshold (e.g., 10–50 cm, the approach taken by Stroeve et al., 2018) and allows us to avoid biasing our results based on the changing location of the ice edge (i.e., we could calculate an increase in ice thickness if we just removed a large area of thin ice). This should be considered when we present our Eastern Arctic (EA) and wider AO results, as they can include significant regions of open water. We do also show the CS-2 results with the raw data masked below 0.5 m, to highlight its impact on our regional analyses. Also, the GSFC data product only produces thickness estimates within a central AO domain, due to their more conservative snow depth assumptions. We thus focus our analyses on three different regions: (i) the central AO, (ii) the Western Arctic (WA, thicker multiyear ice regime), and (iii) the EA (thinner first-year ice regime) as shown in Figure 1.

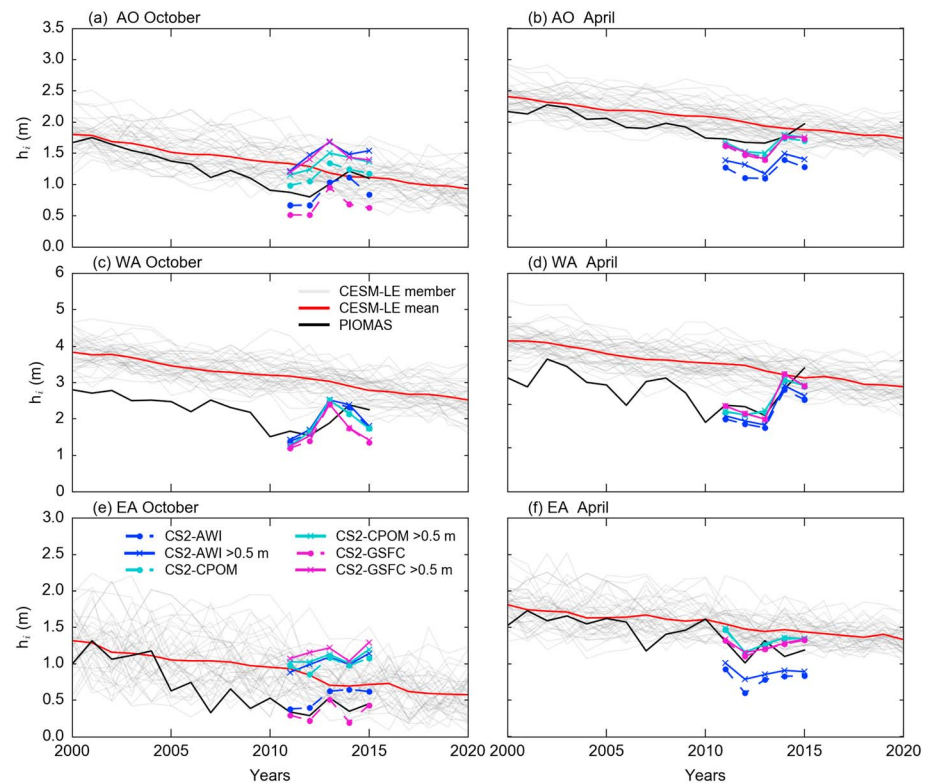


Figure 2. (left) October and (right) April sea ice thickness averaged across the three study regions given in Figure 1 with the Community Earth System Model Large Ensemble (ensemble values in gray, ensemble mean in red), Pan-Arctic Ice-Ocean Modeling and Assimilation System (black line), and CryoSat-2 from Alfred Wegener Institute (blue), Center for Polar Observation and Modeling (cyan), and National Aeronautics and Space Administration Goddard Space Flight Center (magenta) including the data masked below 0.5 m (dashed lines and circles). AO: Arctic Ocean, WA: Western Arctic, EA: Eastern Arctic.

3. Winter Sea Ice Thickness Variability

Maps of the start/end winter ice thickness in the CESM-LE for 2006–2020 (Figure 1) show the simulated winter ice thickness change in CESM-LE and highlight how this is driven by both increases in the thickness of the pack ice and an expansion of the sea ice edge. Figure 1 also shows the thermodynamic/dynamic contribution to this thickness change, demonstrating that across most of the Arctic, thermodynamics drive most of the increase in ice thickness, although dynamics can contribute significantly in some regions. For example, ice growth in the East Greenland Sea and the Labrador Sea is driven by the southward advection of sea ice into these regions. Dynamical ice growth shows only a weak contribution to the total ice growth in our three study regions. Spatial maps of the standard deviation of these terms are given in the supplementary information (Figure S1 in the supporting information). The recent study of Kwok (2015) attempted to estimate empirically the contribution of dynamics/thermodynamics to recent Arctic sea ice mass balance variability using a mass conservation approach; however, this focused more on sea ice melt and convergence through summer, hindering a more direct comparison with this model results.

In Figure 2 we show comparisons of the start (October) and end (April) of winter ice thickness from the CESM-LE, PIOMAS, and the three CS-2 products (AWI, CPOM, and GSFC) across our three study regions. Note that a similar comparison between PIOMAS and CESM-LE was included in the recent study of Labe et al. (2018), focusing mainly on March and September. Here we provide a more detailed regional comparison across our months of interest, also incorporating the various CS-2 products available over the shorter (2011–2015) time period.

In general the CESM-LE, PIOMAS, and CS-2 products show reasonable agreement, although this depends on the region and month of interest, and in some cases the CS-2 product chosen. The CESM-LE October

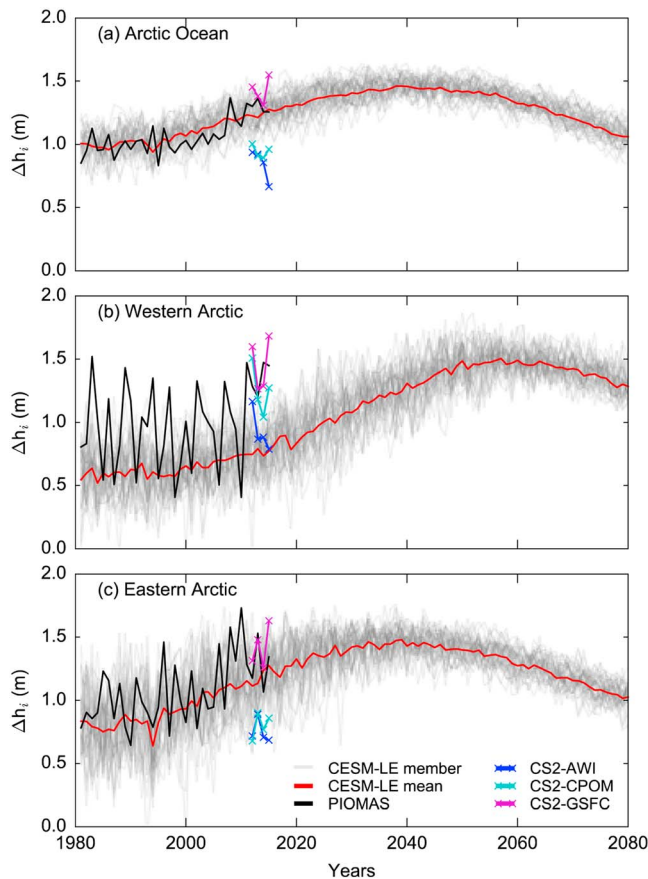


Figure 3. Winter (October to April) sea ice thickness change averaged across our three study regions given in Figure 1 with the Community Earth System Model Large Ensemble (CESM-LE; ensemble values in gray, ensemble mean in red), Pan-Arctic Ice-Ocean Modeling and Assimilation System (PIOMAS; black line), and CryoSat-2 (CS2) from Alfred Wegener Institute (AWI; blue), Center for Polar Observation and Modeling (CPOM; cyan), and NASA Goddard Space Flight Center (GSFC; magenta).

thickness results in the WA region appear to be biased high compared to PIOMAS and CS-2 data. The EA and AO October thickness comparisons show that the PIOMAS thickness estimates are generally consistent with, but at the lower end of, the CESM-LE ensemble spread. The April thickness simulated in CESM-LE suggests a similar, albeit less clear, thickness bias in the WA region compared to PIOMAS and CS-2, but a thickness similar to and consistent with PIOMAS in the AO and EA regions.

The CS-2 products show weaker agreement in the EA region (product differences of ~ 0.5 to 1 m), due in-part to the challenges associated with capturing thinner first-year ice growth in the marginal Arctic seas. The difference between using masked data (below 0.5 m) and filling in the open water/masked data with zero thickness is also high in the EA October results, with differences of 0.5–1 m from this choice of masking approach alone. The spring results show less sensitivity to this masking approach, due to the higher ice concentrations/thicknesses. Much of the calibration/validation of CS-2 sea ice thickness has also been carried out over the WA (e.g., NASA’s Operation IceBridge airborne campaigns and upward looking sonar moorings in the Beaufort Sea), providing a further possible cause of this stronger disagreement in the less constrained EA region. These differences make it challenging to use the CS-2 for model validation, as the choice of observational product can largely determine the interpretation of consistency between the models and observations, thus limiting confidence in prescribing a possible model bias compared to “observations.” In some cases the use of multiple products can be used to provide some increased confidence in the modeled thickness estimates; for example, the CPOM/GSFC products show stronger agreement with PIOMAS and CESM-LE in the April/EA analysis compared to the AWI CS-2 product, which exhibits a clear low bias. The correlation coefficient and root-mean-square differences between PIOMAS and the three CS-2 products are summarized in Table S1 in the supporting information, while maps of the winter thickness/change across the three CS-2 products are given in Figure S2.

The magnitude of the current interannual variability in winter ice thickness across CS-2, PIOMAS, and CESM-LE are all broadly consistent, however, which is encouraging. The recent increase in sea ice thickness from CS-2 in autumn 2013 reported by Tilling et al. (2015) and Kwok (2015) also appears to be within range of the interannual variability in autumn/winter ice thickness in the CESM-LE. The PIOMAS results show significant decreasing trends across all study regions/months over the period 1980–2015. The mean CESM-LE results show similar decreasing trends to PIOMAS, with the strength and significance of the trend varying based on the time period analyzed. We decided not to do a more thorough trend analysis in this study to keep the focus on variability in winter ice growth. The CS-2 period is too short for a trend assessment. We also did not undertake a more detailed investigation into the biases in ice thickness between CESM-LE, PIOMAS, and CS-2. However, Figure S3 shows the reference 2-m air temperature from CESM-LE and the NCEP-R1 reanalysis, which is used to force PIOMAS. In some cases, for example, the April WA results, the thickness bias appears to be related to a clear bias in air temperatures, although in others, for example, the October WA results, no obvious bias in air temperatures is observed between CESM-LE and NCEP-R1 related to the thickness biases.

In Figure 3 we show the observed and simulated winter ice growth estimates, calculated as the difference between the April and October thickness to be consistent with the monthly CS-2 thickness products. Again, maps of the winter thickness change from the three CS-2 products are shown in Figure S2. The winter ice growth in CESM-LE is generally consistent with the PIOMAS ice growth, especially within the AO and EA regions where the PIOMAS results lie clearly within the ensemble spread. The CESM-LE ice growth in the WA region is consistent with, but lower on average than PIOMAS, which may be due to its higher mean October

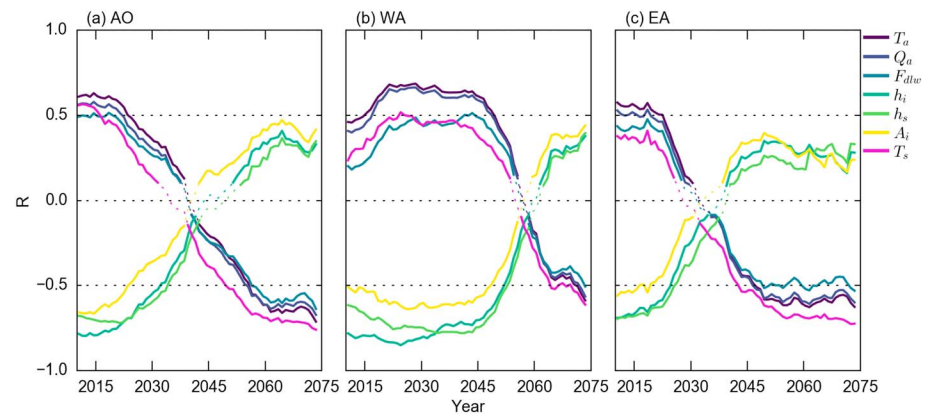


Figure 4. The correlation coefficient between October ice/atmosphere/ocean conditions in the Community Earth System Model Large Ensemble (CESM-LE) and the winter (October–April) thermodynamic Arctic ice growth also from CESM-LE. T_a = 2-m air temperature, Q_a = 2-m specific humidity, F_{dlw} = longwave downwelling, h_i = ice thickness, h_s = snow depth, A_i = ice concentration, T_s = sea surface temperature. Each correlation coefficient (R) is calculated using 10 years of data across the 40 ensemble members. (a–c) The regions are given in Figure 1. The correlations not significant at the 90% confidence level are shown by the lighter, dotted lines.

thicknesses limiting the potential winter ice growth. The CS-2 winter growth results show more significant spread relative to the thickness comparisons. In the WA region, the CPOM/GSFC CS-2 results show a stronger correspondence with PIOMAS, with these ice growths at the higher end of the CESM ensemble spread. In the AO and EA regions, the GSFC CS-2 ice growth estimates show a better correspondence with PIOMAS, which are at the higher end of the CESM-LE ensemble spread, with the CPOM and AWI CS-2 ice growth estimates similar, but at the low end of the CESM-LE spread. The correlation coefficient and root-mean-square differences between PIOMAS and the three CS-2 winter growth estimates are summarized in Table S2, highlighting the relatively low and insignificant correlations between CS-2 and PIOMAS (at the 90% confidence level), but the lower root-mean-square errors between the GSFC CS-2 estimates and PIOMAS compared to the AWI/CPOM products. The short (4 years) time period prevents a more detailed comparison.

A significant increase in ice growth is simulated by PIOMAS in the AO and EA regions over the recent 1980–2015 time period (~10 cm/decade in both regions). CESM-LE shows not only a virtually identical increasing ice trend in these two regions over this time period but also a small but significant increasing trend in the WA region (~5 cm/decade) based on the mean of the 40 ensemble members. CESM-LE also clearly projects a future increase in ice growth in this region. This increase in ice growth extends to ~2,030 in the EA region, ~2,060 in the WA region, and ~2,040 in the AO region. All three regions then show a transition to decreases in ice growth through to the end of the century.

4. Drivers of Winter Ice Growth Variability

Here we assess the drivers of the internal variability in winter ice growth in the CESM-LE and how this is projected to change over the coming decades. Our goal is to understand the drivers of interannual winter ice growth variability—that is, the relative importance of the ice/ocean/atmospheric state—and how we expect this to change in the future on decadal time-scales. Figure 4 shows the correlations between several October ice and atmosphere variables simulated in CESM-LE and the winter (October to April) ice growth.

In the early part of the 21st century, the correlations between the October ice state (thickness, snow depth, and ice concentration) are all strong, significant (>99%), and negative ($R < -0.5$ across all three regions), suggesting that a higher October ice state (i.e., thicker ice and more snow) is strongly related to reduced winter ice growth. This is expected from the negative feedback associated with the insulative nature of sea ice and its overlying snow cover (Bitz & Roe, 2004). Conversely, the correlations between the October atmospheric conditions (air temperature/humidity and downwelling longwave) and the ocean state (sea surface temperature) are moderate/strong and positive ($R \sim 0.5$ across all three regions), suggesting that warmer atmosphere/ocean states are related to increases in winter ice growth. A positive relationship between

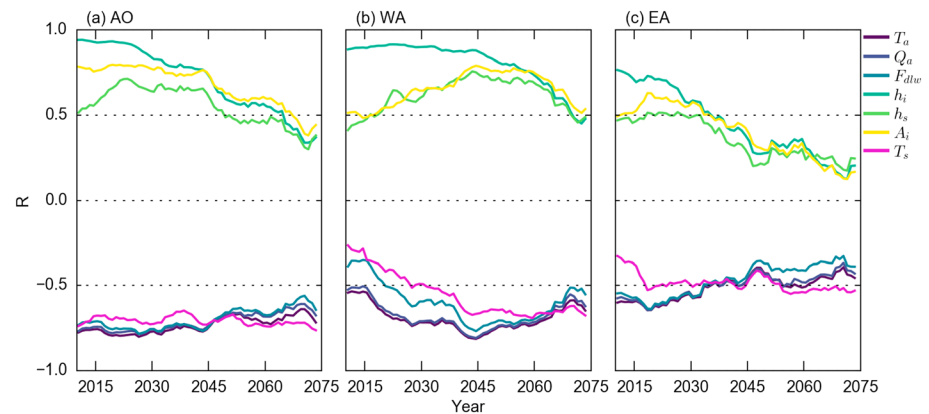


Figure 5. As in Figure 4 but for the correlations between the October ice/atmosphere conditions and the April ice thickness. All correlations are significant at the 90% confidence level.

atmospheric/oceanic conditions that promote ice melt (i.e., warmer air/ocean temperatures) and increased ice growth is counter intuitive. Our interpretation instead is that the October atmospheric forcings/ocean state are strongly coupled with the October ice thickness, which is what more likely drives the winter ice growth variability.

We recognize the challenge in interpretation correlations between variables that are themselves highly coupled, but what is arguably more insightful is that the strength of these correlations reduce and eventually switch in polarity as the simulations progress through the 21st century. This happens first in the EA region, which shows a transition to a moderate but positive correlation ($R \sim 0.4$) between the October ice state and winter ice growth around 2035, with the AO region transition happening ~ 10 years later, and the WA region ~ 20 years later. The atmospheric forcing/ocean state correlations show a virtually identical (but symmetric) response. In this transitioned state, thicker October ice is related with higher winter ice growth and a warmer October atmosphere/ocean state is linked with reduced winter ice growth. Now the October ice state correlations make no physical sense. One interpretation is that the October ice state is related to the October atmospheric forcing, which drives the winter ice growth variability. Another is that the ocean is becoming more significant, and the October ice state is becoming more related to the amount of heat stored in the ocean at the end of the extended melt season that needs to be fluxed away before the winter refreeze can begin—that is, a delayed ice freezeup. In a more open ocean, the near-surface atmosphere and sea surface temperatures are expected to be tightly coupled. In both cases, it appears the negative feedback associated with sea ice thickness reduces in its significance compared to these other processes in future decades. We also carried out an analysis of winter ice growth only for grid cells with an October ice concentration above 15%, which showed increases in winter ice growth through to the end of the century (Figure S4). This suggests that the warming ocean and delayed freezeup is likely to be dominating this response at the end of the century, although the changing location of the ice edge in this approach makes such interpretations challenging.

This transition can be further demonstrated by plotting the correlation coefficient as a function of the mean start-of-winter concentration and thickness across the ensemble members, instead of time (Figure S5), suggesting that this transition happens when the mean October ice thickness reduces to less than 0.5 m and/or the ice concentration reduces to less than 50%, that is, a virtually ice-free October state. The thickness/concentration thresholds seem broadly region independent.

In general these results suggest that as regions of the Arctic become ice free at the end of summer, we expect that the October ice state will become a less useful predictor of the winter ice growth. Note that Stroeve et al. (2018) found a correlation coefficient of $R = -0.82$ between their simulated November ice thickness and the November to April ice growth, but a weakening of this negative correlation in recent years, coincident with the exceptionally warm recent Arctic winters. Their results align with our suggestion that the Arctic may be already transitioning to a state where the amount of ice growth is driven more by the strength of the atmospheric or ocean forcing over variability in the initial ice thickness.

It is important to stress that in the above analysis we are discussing winter ice growth, not the end of winter thickness. Figure 5 shows the correlations between the October ice/atmosphere CESM-LE variables and the April ice thickness in our three study regions.

The correlations between the October ice state (especially thickness) and April ice thickness are even stronger in the current time period than those for the winter ice growth shown in Figure 4, with the AO and WA regions showing $R > 0.9$. In Figure 5 we also see that despite the existence and weakening negative feedback, the ability to predict the April ice thickness using October ice state information generally weakens, but the correlations remain positive, as we transition to a warmer Arctic with a diminished ice cover. Indeed the October atmosphere/ocean state information eventually becomes a better (higher R value) predictor of April ice thickness than the initial ice state.

5. Conclusions

In this study we explored winter Arctic sea ice thickness and growth variability using data from a fully coupled climate model, an ice-ocean reanalysis and satellite altimetry observations. The combination of models and observations allows us to better assess current winter thickness and growth variability and provide needed context for simulated projections over the coming decades. While the period of satellite altimetry derived sea ice thickness data is short, more reliable thickness products are needed to better constrain current model estimates. The CESM-LE projects an increase in winter Arctic sea ice growth over the coming decades, likely due to the negative feedback associated with thinner/less insulated sea ice. PIOMAS and CESM-LE suggest that this increase is already underway in the Eastern Arctic, with the Western Arctic expected to increase its ice growth over the coming decades as the mean winter ice state continues to decline. By the middle of the century, increases in atmospheric forcing and/or a warming of the ocean are expected to dominate over this negative feedback and promote declines in Arctic sea ice growth. Our results suggest that this negative feedback process becomes less significant as the mean October ice state declines to near ice-free conditions (~0.5-m thickness and/or 50% concentration), broadly independent of the region analyzed. Thus, the negative feedback mechanism increasing ice growth appears unlikely to be sufficient in preventing an ice-free Arctic this century. Despite this, some predictive skill should still remain in using October (start of winter) thickness estimates to predict ice conditions at the end of winter.

Acknowledgments

We would like to thank the NSF Polar Programs for supporting this collaboration between modeling and observational sea ice researchers (NSF 1417642). M. Holland acknowledges support from NOAA Award NA15OAR4310167. We also acknowledge the CESM LE Community Project and supercomputing resources provided by NSF/NCAR CISL/Yellowstone. CESM-LE data were obtained from <http://www.cesm.ucar.edu/projects/community-projects/LENS/data-sets.html>. The PIOMAS thickness data were obtained from http://psc.apl.uw.edu/research/projects/arctic-sea-ice-volume-anomaly/data/model_grid. The NASA GSFC CS-2 Arctic sea ice thickness data were obtained through the National Snow and Ice Data Center <https://nsidc.org/data/RDEFT4>. The CPOM thickness data were obtained from <http://www.cpom.ucl.ac.uk/csopr/seaice.html>. The AWI thickness data were obtained from <http://data.seaiceportal.de/data/cs2smos/version1.3/n/> (and can be accessed through the online portal <http://data.meereisportal.de>).

References

- Bitz, C. M., & Roe, G. H. (2004). A mechanism for the high rate of sea ice thinning in the Arctic Ocean. *Journal of Climate*, 17(18), 3623–3632. [https://doi.org/10.1175/1520-0442\(2004\)017<3623:AMFTHR>2.0.CO;2](https://doi.org/10.1175/1520-0442(2004)017<3623:AMFTHR>2.0.CO;2)
- Boisvert, L. N., Petty, A. A., & Stroeve, J. C. (2016). The impact of the extreme winter 2015/16 Arctic cyclone on the Barents-Kara seas. *Monthly Weather Review*, 144(11), 4279–4287. <https://doi.org/10.1175/MWR-D-16-0234.1>
- Carmack, E. C., Yamamoto-Kawai, M., Haine, T. W. N., Bacon, S., Bluhm, B. A., Lique, C., et al. (2016). Freshwater and its role in the Arctic Marine System: Sources, disposition, storage, export, and physical and biogeochemical consequences in the Arctic and global oceans. *Journal of Geophysical Research: Biogeosciences*, 121, 675–717. <https://doi.org/10.1002/2015JG003140>
- Cullather, R. I., Lim, Y.-K., Boisvert, L. N., Brucker, L., Lee, J. N., & Nowicki, S. M. J. (2016). Analysis of the warmest Arctic winter, 2015–2016. *Geophysical Research Letters*, 43, 10,808–10,816. <https://doi.org/10.1002/2016GL071228>
- Graham, R. M., Cohen, L., Petty, A. A., Boisvert, L. N., Rinke, A., Hudson, S. R., et al. (2017). Increasing frequency and duration of Arctic winter warming events. *Geophysical Research Letters*, 44, 6974–6983. <https://doi.org/10.1002/2017GL073395>
- Holland, M. M., Bailey, D. A., Briegleb, B. P., Light, B., & Hunke, E. (2012). Improved sea ice shortwave radiation physics in CCSM4: The impact of melt ponds and aerosols on Arctic Sea ice. *Journal of Climate*, 25(5), 1413–1430. <https://doi.org/10.1175/JCLI-D-11-00078.1>
- Holland, M. M., Serreze, M. C., & Stroeve, J. (2010). The sea ice mass budget of the Arctic and its future change as simulated by coupled climate models. *Climate Dynamics*, 34(2–3), 185–200. <https://doi.org/10.1007/s00382-008-0493-4>
- Hunke, E. C., & Lipscomb, W. H. (2010). *CICE: the Los Alamos sea ice model documentation and software user's manual version 4.1*. Los Alamos: T-3 fluid dynamics group, Los Alamos National Laboratory.
- Hurrell, J. W., Holland, M. M., Gent, P. R., Ghan, S., Kay, J. E., Kushner, P. J., et al. (2013). The Community Earth System Model: A framework for collaborative research. *Bulletin of the American Meteorological Society*, 94(9), 1339–1360. <https://doi.org/10.1175/BAMS-D-12-00121.1>
- Jahn, A., Kay, J. E., Holland, M. M., & Hall, D. M. (2016). How predictable is the timing of a summer ice-free Arctic? *Geophysical Research Letters*, 43, 9113–9120. <https://doi.org/10.1002/2016GL070067>
- Kay, J. E., Deser, C., Phillips, A., Mai, A., Hannay, C., Strand, G., et al. (2015). The Community Earth System Model (CESM) Large Ensemble Project: A community resource for studying climate change in the presence of internal climate variability. *Bulletin of the American Meteorological Society*, 96(8), 1333–1349. <https://doi.org/10.1175/BAMS-D-13-00255.1>
- Kurtz, J. C., & Harbeck, J. (2017). *CryoSat-2 level 4 sea ice elevation, freeboard, and thickness, version 1*. Boulder, Colorado USA: NASA DAAC at the National Snow and Ice Data Center. <https://doi.org/10.5067/96J00KIFDAS8>
- Kwok, R. (2015). Sea ice convergence along the Arctic coasts of Greenland and the Canadian Arctic Archipelago: Variability and extremes (1992–2014). *Geophysical Research Letters*, 42, 7598–7605. <https://doi.org/10.1002/2015GL065462>
- Kwok, R., & Rothrock, D. A. (2009). Decline in Arctic Sea ice thickness from submarine and ICESat records: 1958–2008. *Geophysical Research Letters*, 36, L15501. <https://doi.org/10.1029/2009GL039035>

- Labe, Z., Magnusdottir, G., & Stern, H. (2018). Variability of Arctic Sea-ice thickness using PIOMAS and the CESM large ensemble. *Journal of Climate*, 31(8), 3233–3247. <https://doi.org/10.1175/JCLI-D-17-0436.1>
- Lindsay, R., & Schweiger, A. (2015). Arctic Sea ice thickness loss determined using subsurface, aircraft, and satellite observations. *The Cryosphere*, 9(1), 269–283. <https://doi.org/10.5194/tc-9-269-2015>
- Markus, T., Stroeve, J. C., & Miller, J. (2009). Recent changes in Arctic Sea ice melt onset, freezeup, and melt season length. *Journal of Geophysical Research*, 114, C12024. <https://doi.org/10.1029/2009JC005436>
- Notz, D., & Marotzke, J. (2012). Observations reveal external driver for Arctic sea-ice retreat. *Geophysical Research Letters*, 39, L08502. <https://doi.org/10.1029/2012GL051094>
- Notz, D., & Stroeve, J. (2016). Observed Arctic Sea-ice loss directly follows anthropogenic CO₂ emission. *Science*, 354. <https://doi.org/10.1126/science.aag2345>
- Perovich, D. K., Light, B., Eicken, H., Jones, K. F., Runciman, K., & Nghiem, S. V. (2007). Increasing solar heating of the Arctic Ocean and adjacent seas, 1979–2005: Attribution and role in the ice-albedo feedback. *Geophysical Research Letters*, 34, L19505. <https://doi.org/10.1029/2007GL031480>
- Petty, A. A., Stroeve, J. C., Holland, P. R., Boisvert, L. N., Bliss, A. C., Kimura, N., & Meier, W. N. (2018). The Arctic Sea ice cover of 2016: A year of record-low highs and higher-than-expected lows. *The Cryosphere*, 12(2), 433–452. <https://doi.org/10.5194/tc-12-433-2018>
- Polyakov, I. V., Pnyushkov, A. V., Alkire, M. B., Ashik, I. M., Baumann, T. M., Carmack, E. C., et al. (2017). Greater role for Atlantic inflows on sea-ice loss in the Eurasian Basin of the Arctic Ocean. *Science*, 356(6335), 285–291. <https://doi.org/10.1126/science.aai8204>
- Ricker, R., Hendricks, S., Girard-Arduin, F., Kaleschke, L., Lique, C., Tian-Kunze, X., et al. (2017). Satellite-observed drop of Arctic sea-ice growth in winter 2015–2016. *Geophysical Research Letters*, 44, 3236–3245. <https://doi.org/10.1002/2016GL072244>
- Ricker, R., Hendricks, S., Kaleschke, L., Tian-Kunze, X., King, J., & Haas, C. (2017). A weekly Arctic Sea-ice thickness data record from merged CryoSat-2 and SMOS satellite data. *The Cryosphere*, 11(4), 1607–1623. <https://doi.org/10.5194/tc-11-1607-2017>
- Schweiger, A., Lindsay, R., Zhang, J., Steele, M., Stern, H., & Kwok, R. (2011). Uncertainty in modeled Arctic Sea ice volume. *Journal of Geophysical Research*, 116, C00D06. <https://doi.org/10.1029/2011JC007084>
- Stroeve, J. C., Schroder, D., Tsamados, M., & Feltham, D. (2018). Warm winter, thin ice? *The Cryosphere*, 12(5), 1791–1809. <https://doi.org/10.5194/tc-12-1791-2018>
- Stroeve, J. C., Serreze, M. C., Holland, M. M., Kay, J. E., Malanik, J., & Barrett, A. P. (2011). The Arctic's rapidly shrinking sea ice cover: A research synthesis. *Climatic Change*, 110(3–4), 1005–1027. <https://doi.org/10.1007/s10584-011-0101-1>
- Tilling, R. L., Ridout, A., & Shepherd, A. (2017). Estimating Arctic Sea ice thickness and volume using CryoSat-2 radar altimeter data. *Advances in Space Research*, 62(6), 1203–1225. <https://doi.org/10.1016/j.asr.2017.10.051>
- Tilling, R. L., Ridout, A., Shepherd, A., & Wingham, D. J. (2015). Increased Arctic Sea ice volume after anomalously low melting in 2013. *Nature Geoscience*, 8(8), 643–646. <https://doi.org/10.1038/ngeo2489>
- Tsamados, M., Feltham, D., Petty, A., Schroeder, D., & Flocco, D. (2015). Processes controlling surface, bottom and lateral melt of Arctic Sea ice in a state of the art sea ice model. *Philosophical Transactions of the Royal Society A*, 373(2052). <https://doi.org/10.1098/rsta.2014.0167>
- Wingham, D. J., Francis, C. R., Baker, S., Bouzinac, C., Brockley, D., Cullen, R., et al. (2006). CryoSat: A mission to determine the fluctuations in Earth's land and marine ice fields. *Advances in Space Research*, 37(4), 841–871. <https://doi.org/10.1016/j.asr.2005.07.027>
- Zhang, J., & Rothrock, D. A. (2003). Modeling Global Sea ice with a thickness and enthalpy distribution model in generalized curvilinear coordinates. *Monthly Weather Review*, 131(5), 845–861. [https://doi.org/10.1175/1520-0493\(2003\)131<0845:MGSIIWA>2.0.CO;2](https://doi.org/10.1175/1520-0493(2003)131<0845:MGSIIWA>2.0.CO;2)
- Zygmuntowska, M., Rampal, P., Ivanova, N., & Smedsrud, L. H. (2014). Uncertainties in Arctic sea ice thickness and volume: new estimates and implications for trends. *The Cryosphere*, 8(2), 705–720. <https://doi.org/10.5194/tc-8-705-2014>